JBUON 2020; 25(5): 2482-2489
ISSN: 1107-0625, online ISSN: 2241-6293 • www.jbuon.com
Email: editorial_office@jbuon.com

ORIGINAL ARTICLE

Gene expression profiles and protein-protein interaction networks in neuroblastoma with *MEIS2* depletion

Xin-Qian Hu[1]*, Ze-An Weng[2]*, Ying-Feng Xia[1], Yun-Hong Zha[1]

[1]Institute of Neural Regeneration and Repair and Department of Neurology, First People's Hospital of Yichang, Three Gorges University, Yichang 443000, China. [2]First Clinical Medical College of Jinan University, Guangzhou 510630, China.

*These authors contributed equally to this work.

Summary

Purpose: *The purpose of the present study was to identify differential gene expressions (DEGs) and key pathways in neuroblastoma with MEIS2 depletion through bioinformatics.*

Methods: *The microarray gene expression dataset GSE56003 was downloaded from the Gene Expression Omnibus (GEO) database. DEGs were identified using Gene Level RMA sketch and Transcriptome Analysis Console. Gene ontology (GO) function and KEGG pathway enrichment analysis of DEGs were performed using the DAVID online tool. Protein-protein interaction (PPI) networks were constructed by mapping the DEGs onto Cytoscape software. MCODE algorithm was used to select the module and Centiscape was used to screen the hub genes. The Kaplan-Meier survival curves was utilized to show the correlation of specific gene expressions and the survival situation of NB patients.*

Results: *A total of 1352 DEGs were identified in neuroblastoma with MEIS2 depletion, which were mainly enriched during the cell cycle, DNA replication, and DNA repair. CDK2, RAD51, BRCA1, and MCM3 were selected as hub genes that have the potential as novel therapeutic targets for neuroblastoma.*

Conclusion: *This study revealed the hub genes and pathway involved in neuroblastoma with MEIS2 knockdown, which offered new insights into the molecular networks underlying MEIS2 depletion in neuroblastoma. Additionally, this study provided a valuable resource of potential biomarkers and therapeutic targets.*

Key words: *neuroblastoma, MEIS2 depletion, hub genes, protein-protein interaction networks*

Introduction

Neuroblastoma originates from the neural crest and is the most common malignant tumor in children. Moreover, it was reported that the incidence rates in Asian/Pacific Islanders is 6.3 per 1,000,000 persons aged 0–19 years in 2000. The median age at the time of diagnosis is approximately 19 months, which ranges from an intrauterine fetus to patients 19 years old [1]. Several genomic abnormalities, such as MYCN amplification, mutations in ALK and ATRX, and genomic rearrangements in TERT genes, have accounted for promoting the abnormal proliferation and metastasis of neuroblastoma [2]. Typically, a palpable abdominal mass is considered to be the first symptom, but some children also present with generalized bone pain, malaise, fever, and irritability [3]. Diagnosis usually depends on imaging and biopsy [4]. Though the current treatment methods mainly include surgical resection, induction chemotherapy, autologous hematopoietic stem cell transplantation and maintenance treatment, the prognosis remains poor, because of tumor recurrence and metastasis [5]. Therefore, exploring the molecular mechanisms underlying

Corresponding author: Yun-Hong Zha, PhD. Institute of Neural Regeneration and Repair and Department of Neurology, First People's Hospital of Yichang, 4 Hudi Rd, Yichang 443000, China.
Tel: +86 717 6222800, Email: yzha7808@ctgu.edu.cn
Received: 04/03/2020; Accepted: 23/03/2020

neuroblastoma is expected to provide a more in-depth understanding for new targets of antitumor drugs.

The Meis Homeobox 2 (*MEIS2*) gene is a member of TALE homeobox gene family. *MEIS2* is primarily involved during embryonic early development and is implicated in the pathogenesis of human cancer [6]. *MEIS* has been observed to directly bind to Pbx. The resulting Meis/Pbx complex is mainly involved in the development of several organs, for example, limbs, heart, lens, pancreas, and hindbrain [3]. *MEIS2* is highly expressed in patients with acute lymphoblastic leukemia (AML). Additionally, *MEIS2* is considered to be an oncogenic partner with AML1-ETO in AML [7]. Also, *MEIS* plays a significant role in MN1-induced leukemia. High expression levels of the *MEIS1* and *MEIS2* gene products have also been identified in a panel of neuroblastoma cell lines [8]. Our previous study [3] identified that high expression levels of *MEIS2* is inversely correlated with prognosis in neuroblastoma patients. *MEIS2* can regulate neuroblastoma cell survival and proliferation through transcriptional control of M-phase progression, which suggest that *MEIS2* expression plays an essential role in neuroblastoma proliferation and metastasis [3].

The molecular basis of *MEIS2* gene's mechanism of action in tumorigenesis remains unknown. Several studies have used gene expression profiling techniques in knocking down *MEIS2* to identify the effect of tumorigenesis where several hundred differentially expressed genes were identified. However, few studies focused on the *MEIS2*-involved pathways and the protein-protein interaction networks. In order to screen potential hub genes involved in the development of neuroblastoma pathology as well as to identify varying molecular mechanisms and pathways related to neuroblastoma with *MEIS2* depletion, bioinformatics analysis was performed to a microarray gene expression dataset GSE56003, which was downloaded from the Gene Expression Omnibus (GEO) database (https://www.ncbi.nlm.nih.gov/geo/). Gene ontology (GO) enrichment analysis and Kyoto Encyclopedia of Genes and Genomes (KEGG) pathway analysis was performed, and a protein-protein interaction (PPI) network was constructed by mapping DEGs to human PPI data. Our research established an interrelationship between DEGs, KEGG pathways, and protein-protein interaction networks. Such an interrelationship will help identifying different molecular mechanisms involved in the pathogenesis of neuroblastoma with the hope of providing a valuable resource for potential biomarkers and therapeutic targets.

Methods

Microarray data collection and preprocessing

We searched GEO (www.ncbi.nlm.nih.gov/geo/) [9] for the study associated with *MEIS2*. Two datasets were related to a *MEIS2* depletion group and a negative control group in human neuroblastoma BE (2)-C cells. There are three inclusion criteria shown as follows: (1) The data were genome-wide microarray data; (2) *MEIS2* depletion; (3) Complete microarray raw or normalized data were accessed. Finally, GSE56003 was utilized for further analysis. The data was based upon [HuGene-1_0-st] Affymetrix Human Gene 1.0 ST Array Plate. The dataset contained six samples, including three BE(2)-C cells infected with lentiviruses expressing sh*MEIS2*-43 for 48 h, and the other three negative control groups infected with lentiviruses expressing shGFP. The mode of analysis used was the Gene Level RMA sketch. Gene expression values and clustering were completed using the Transcriptome Analysis Console (Affymetrix, Inc., Santa Clara, CA, USA). An adjusted p value <0.05 and |log-FC|>1.5 were set as the cut-off criterion to screen DEGs.

Functional and pathway enrichment analysis of MEIS2-specific DEGs

Gene Ontology (GO) (http://geneontology.org/) [10] is a bioinformatics tool, which is mainly used to annotate genes and gene products. It mainly consists of three categories: cell composition, molecular function, and biological process. The Kyoto Encyclopedia of Genes and Genomes (KEGG) [11] is a database resource for integration and interpretation of genomic information as well as

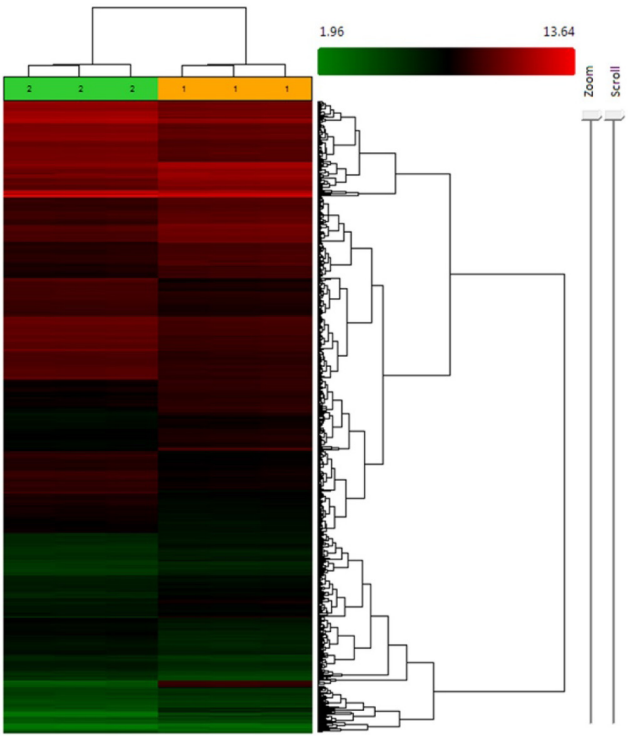

Figure 1. Hierarchical clustering analysis of differentially expressed genes. Red represents the higher levels of gene expression; blue represents lower levels of gene expression.

chemical and systems information. GO and KEGG analyses were available in the DAVID database (https://david.ncifcrf.gov/), which were integral functional annotation tools to reveal the biological significance behind a large list of genes. P value <0.05 was set as the cut-off criterion.

Construction of protein-protein interaction (PPI) network

The STRING database (http://string-db.org/) [12] is developed and managed by EMBL, SIB, and UZH, including various protein interaction databases. The STRING 9.1 online tool was used to construct an interaction network of DEGs with the thresholds of required confidence (combined score) >0.4.

The PPI networks and screening of hub genes

The network data obtained from online STRING 9.1 software were imported into Cytoscape software version 3.5.1 [13]. The corresponding network was further visually analyzed. The CentiScaPe 2.2 plug-in was used to calculate the topology of the network, each node, and screen key nodes. The hub genes were selected based on the values of degree and betweenness between nodes. In our study, nodes with both degree and betweenness values greater than the mean, were considered as key nodes.

The PPI networks and module selection

The PPI networks were visualized by Cytoscape software. The Molecular Complex Detection (MCODE) plug-in was used to select important functional modules of protein interaction networks. We used the MCODE plug-in default parameters: degree cut-off = 10, node score cut-off = 0.2, k-core = 2, and max. depth = 100. Moreover, the BiNGO plug-in was used to perform the functional and pathway enrichment analyses of DEGs in each module with the threshold of p value <0.05.

Evaluation of gene expression correlation with survival in NB patients

To evaluate the correlation of specific gene expressions and the survival situation of NB patients, we applied online datasets to produce Kaplan-Meier survival curves. The R2: Genomics Analysis and Visualization Platform (http://hgserver1.amc.nl/cgi-bin/r2/main.cgi) and Tumor Neuroblastoma -SEQC-498-RPM-seqcnb1 datasets were utilized to measure the expression of critical genes in NB biopsies.

Results

Identification of DEGs and hierarchical clustering analysis

In total, 1352 DEGs between the *MEIS2* knockdown group and the control group were identified, which included 704 downregulated DEGs and 648 upregulated DEGs. Following hierarchical cluster-

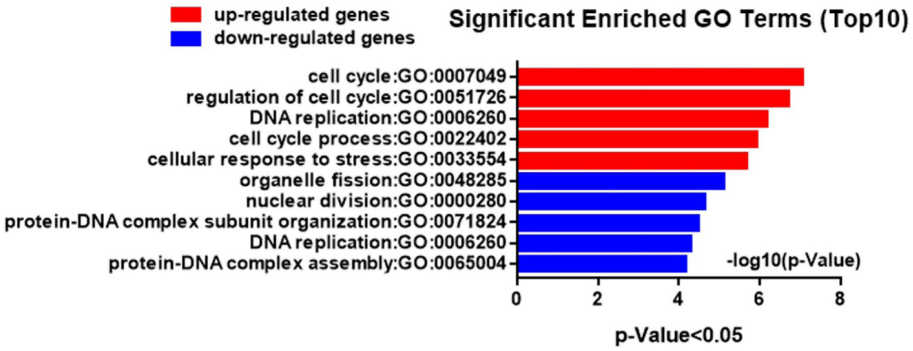

Figure 2. Gene Ontology analysis and significant enriched GO terms of DEGs.

Table 1. GO functional enrichment analysis of up- and downregulated DEGs

Category	*Term*	*Description*	*Count*	*p value*
Up-regulated				
GOTERM_BP_FAT	GO:0007049	cell cycle	89	8.746E-8
GOTERM_BP_FAT	GO:0051726	regulation of cell cycle	60	1.904E-7
GOTERM_BP_FAT	GO:0006260	DNA replication	27	6.614E-7
GOTERM_BP_FAT	GO:0022402	cell cycle process	73	1.202E-6
GOTERM_BP_FAT	GO:0033554	cellular response to stress	88	2.135E-6
Down-regulated				
GOTERM_BP_FAT	GO:0048285	organelle fission	40	7.617E-6
GOTERM_BP_FAT	GO:0000280	nuclear division	37	2.315E-5
GOTERM_BP_FAT	GO:0071824	protein-DNA complex subunit organization	22	3.371E-5
GOTERM_BP_FAT	GO:0006260	DNA replication	23	5.091E-5
GOTERM_BP_FAT	GO:0065004	protein-DNA complex assembly	20	7.039E-5

ing analysis, there were two distinct gene clusters identified, including the *MEIS2* depletion cluster and control cluster (Figure 1). These results suggest that there were two different gene expression patterns with marked color differences, which were available for use to distinguish between the *MEIS2* depletion samples and the control samples.

GO enrichment analysis and KEGG pathway enrichment analysis of DEGs

The GO and KEGG pathway enrichment of the identified DEGs were analyzed with the DAVID tool. GO biological process (BP) analysis indicated that upregulated DEGs were mainly involved in the mitotic cell cycle, DNA replication, and DNA repair. The downregulated DEGs were mainly enriched in those relating to cell division and DNA replication (Figure 2, Table 1). In addition, KEGG analysis showed that the upregulated DEGs were mainly enriched in alcoholism, Fanconi anemia, and the cell cycle, while downregulated DEGs were mainly enriched in Taste transduction, Homologous recombination, and Systemic lupus erythematosus (Figure 3, Table 2).

MEIS2-specific PPI network construction and hub gene identification

The DEGs in *MEIS2*-knockdown cells were analyzed with STRING. The PPI network was constructed with 991 nodes and 3942 degrees. Furthermore, CentiScaPe software, which calculated topological characteristics of each node, was used to gain an in-depth understanding of the biological characteristics of the PPI network, but not including unrelated proteins. When the network diameter was 10, the average distance of the network was 3.34. The maximum node degree was 90, the minimum was 1, with an average of 10.95. The maximum betweenness was 52712.57, the minimum was 0, with an average of 1733.12. Proteins with high values were more important in the network, suggesting they play a central role in maintaining the functionality and the coherence of signaling mechanisms. In our PPI network, hub proteins with high node degree and betweenness (> Means) were CDK2, RAD51, BRCA1, MCM3, JUN, ACACA, RFC4, AURKB, EXO1, DTL, MELK, HIST1H2BM, RRM2, KNTC1, TYMS, BLM, HIST1H2BB, FANCI, FOLE2 and UBE2T (Table 3).

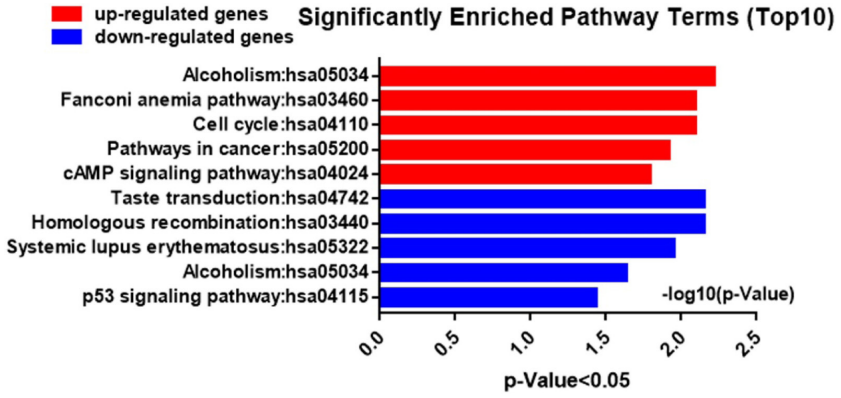

Figure 3. Significantly enriched pathway terms of DEGs.

Table 2. The enriched KEGG pathway of DEGs

Category	*Term*	*Description*	*Count*	*p value*
Up-regulated				
KEGG_PATHWAY	hsa05034	Alcoholism	14	0.006
KEGG_PATHWAY	hsa03460	Fanconi anemia pathway	7	0.008
KEGG_PATHWAY	hsa04110	Cell cycle	11	0.008
KEGG_PATHWAY	hsa05200	Pathways in cancer	23	0.012
KEGG_PATHWAY	hsa04024	cAMP signaling pathway	14	0.016
Down-regulated				
KEGG_PATHWAY	hsa04742	Taste transduction	6	0.007
KEGG_PATHWAY	hsa03440	Homologous recombination	5	0.007
KEGG_PATHWAY	hsa05322	Systemic lupus erythematosus	10	0.011
KEGG_PATHWAY	hsa05034	Alcoholism	11	0.023
KEGG_PATHWAY	hsa04115	p53 signaling pathway	6	0.036

PPI network and module selection

Based on the STRING output, there were 342 genes with their degree ≥10 module score ≥3. Through the plug-in MCODE, two significant modules were selected with MCODE score ≥20, nodes ≥20, and edges ≥10 (Figure 4). Functional enrichment analysis indicated that the hub genes in module one were significantly enriched in DNA replication, cell cycle, and DNA repair, while the hub genes in module two did not produce any classification for the selected nodes.

Table 3. Significantly key genes using CentiScaPe software

Name	*Degree*	*Betweenness*
CDK2	90	29763
RAD51	80	13391
BRCA1	79	23665
MCM3	70	12171
JUN	68	50741
ACACA	66	52712
RFC4	66	8194
AURKB	66	6519
EXO1	63	2894
DTL	59	5927
MELK	57	9098
HIST1H2BM	56	9402
RRM2	56	8191
KNTC1	56	7711
TYMS	55	4854
BLM	55	2938
HIST1H2BB	54	8121
FANCI	54	2930
FOLE2	52	1711
UBE2T	51	8810

The high expression of CDK2, RAD51, BRCA1, and MCM3 indicated poor survival in neuroblastoma patients

The definition of high and low expression was computer-generated based on the threshold that provided the best distinction between the two populations of gene expression. High expression of CDK2, RAD51, BRCA1 and MCM3 indicated a significant decrease in overall patient survival (Figure 5).

Discussion

In this study, the microarray data were used to find hub genes related to *MEIS2* depletion. *MEIS2* was considered a cofactor of the *hox* gene, mainly involved in early embryonic development and tumor proliferation.

In our study, a total of 1352 DEGs, including 648 upregulated genes and 704 downregulated genes were screened with bioinformatics. The upregulated DEGs were mainly involved in the mitotic cell cycle, DNA replication, and DNA repair, while the downregulated DEGs were mainly enriched in those relating to cell division and DNA replication. Moreover, we identified high degree genes including *CDK2, RAD51, BRCA1, MCM3, JUN, ACACA, RFC4, AURKB, EXO1, DTL, MELK, HIST1H2BM, RRM2, KNTC1, TYMS, BLM, HIST1H2BB, FANCI, FOLE2* and *UBE2T* with constructing the PPI and CentiScaPe software. By means of modules analysis, the hub genes in module were significantly enriched in DNA replication, cell cycle and DNA repair.

It has been assumed that mutagenesis plays a pivotal part in the progression phase of tumori-

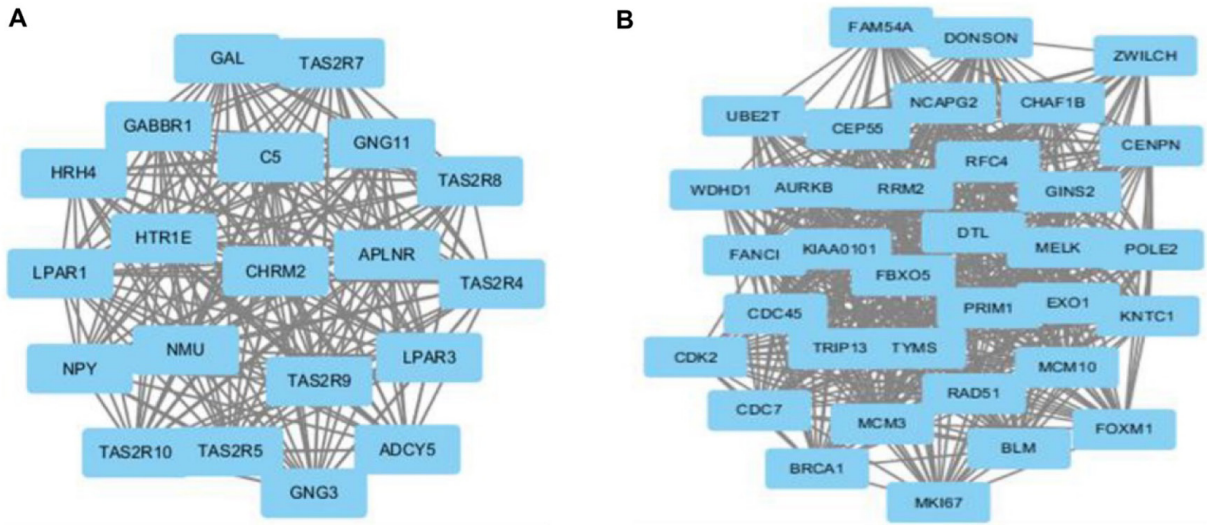

Figure 4. Two significant modules selected from the PPI network. **A:** *Module 1* **B:** *Module 2.*

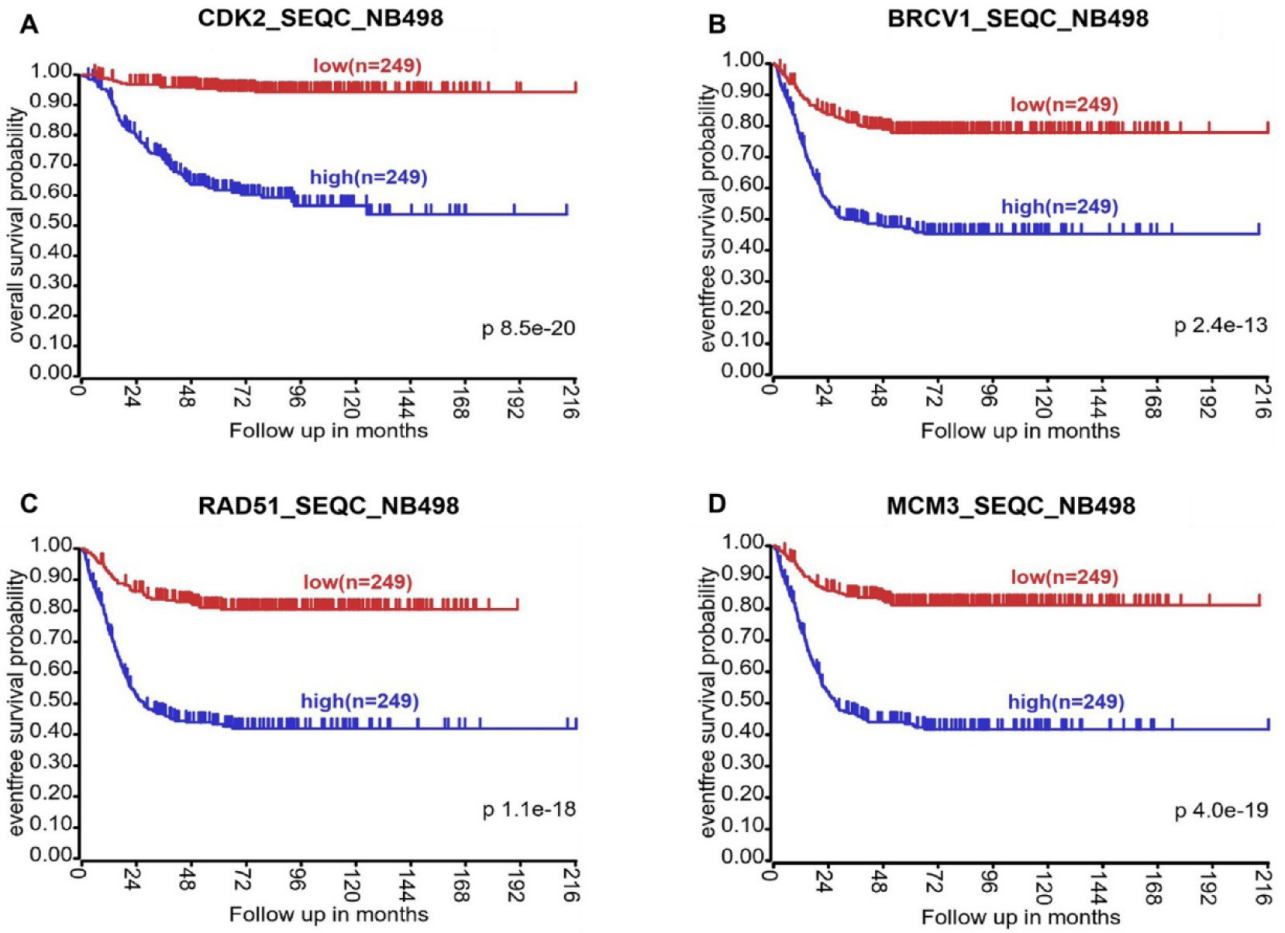

Figure 5. Kaplan-Meier survival curves for the SEQC cohort of 498 neuroblastoma patients based on the average mRNA expression of the CDK2 **(A)** RAD51 **(B)**, BRCA1 **(C)** and MCM3 **(D)** gene signature, with log-rank test P value indicated. Curves were generated with R2: Genomics Analysis and Visualization Platform using Tumor Neuroblastoma-SEQC-498-RPM-seqcnb1 dataset.

genesis. The resulting mutations, which accumulate during abnormal cell division, have shown to be a result of two different mechanisms: acquired variation in DNA replication or shortage in DNA repair. Several studies support the view of disordered DNA replication in neuroblastoma. Cell cycle regulatory proteins ensure accurate DNA replication in a cell-controlled level. It is reported that the overexpression and/or distortion of cell cycle regulatory proteins are involved in the pathogenesis of neuroblastoma [14]. The DNA repair process is a complex system consisting of diverse processes including error-prone repair, base-excision repair and mismatch repair. These processes are activated as a result of DNA damage stimuli. Dysregulation of one or more DNA repair pathways usually lead to carcinogenesis [15].

CDK2 is a member of phase-specific cyclin-dependent kinases, which is involved in both G1/S transition and initiation of DNA replication. A recent study suggested that siRNA knockdown of CDK2 resulted in G1 phase arrest in mouse embryonic stem cells [16]. The pharmacological evidence suggested that overexpression of CDK2 causes abnormal cell-cycle regulation, which directly results in hyperproliferation of cancer cells [17]. Abnormal activation of CDKs has been shown to contribute to tumor cell proliferation and growth in many cancers, including neuroblastoma. Ainaciclib, a novel multiple-CDK inhibitor, inhibits NB cell proliferation and induces cell cycle arrest in many types of neuroblastoma cell lines [18] . On the one hand, CDK2 knockdown inhibited cell proliferation and growth in all neuroblastoma cell lines and cell cycle analysis at 3 days after CDK2 siRNAs showed accumulation of cells in G1/G0 phase in most cell lines [19]. On the other hand, *MEIS2* depletion can induce M-phase arrest. As mentioned above, upregulated *CDK2* after *MEIS2* silencing may accelerate neuroblastoma progression.

RAD51 is a critical enzyme that plays essential roles in DNA double-strand break (DSB) repair by the homologous recombination pathway [20]. RAD51 is overexpressed in many kinds of

cancer cell lines and is related to poor prognosis, because RAD51 protein significantly promotes the cell cycle transition of the G0/G1 phase and the expression of RAD51 in tumor cells, possibly increasing the resistance to anticancer agents [21]. A case-control study found that overexpression of RAD51 was relevant to the progression of thyroid carcinoma. High RAD51 expression indicated later stages, poor tissue differentiation, large tumor size, greater possibility of lymph node metastasis, and distant metastasis [22]. At the same time, RAD51 is overexpressed in esophageal squamous carcinoma cells. RAD51 interacts with *CHK1* with its DMC1 domain to increase the expression of CHK1, which subsequently promotes its oncogenic role in tumorigenesis [23].

BRCA1 was first discovered in 1994 and has been identified to maintain genetic stability via DNA damage response pathways. Homology-directed repair (HDR) consist of homologous recombination (HR) and single-strand annealing (SSA). BRCA1 regulates homology-directed repair (HDR) of DNA double-strand breaks [24]. BRCA1 can physically interact with p53 and co-regulate its transcriptional targets, shifting cellular outcomes towards cell cycle arrest. A study detected the presence of BRCA1 upstream of the transcriptional start site of *MEIS2*, and knockdown of BRCA1 can down-regulate *MEIS2* expression [25]. This requires further investigation to explore the regulation mechanism between the two genes.

Minichromosomal maintenance (MCM) proteins play a central role in DNA synthesis in prokaryotic and eukaryotic cells. MCM proteins form Mcm2-7 hexamers that act as replicative DNA helicase for quality control of DNA replication origin licensing [26]. The ATM and ATR checkpoint kinases directly interact with three members of the MCM complex to regulate DNA replication [27]. MCM3 is overexpressed in various cancers. Furthermore, increased expression of MCM3 genes is an independent biomarker of poor prognosis.

Conclusions

In our study, a variety of bioinformatics methods were performed, such as the construction of a PPI network, hub gene analysis, module analysis of the PPI network, and the prediction of transcription factor to discover the relationship between the significance of genes and several topological properties in the human PPI network. We have detected gene expression changes that occurred in human neuroblastoma BE(2)-C cells with *MEIS2* depletion. According to this, gene expression data of the *MEIS2* depletion group and negative control group were used to screen DEGs related to neuroblastoma. Several kinds of bioinformatic tools were used to discover hub genes, enriched GO terms and KEGG pathways. GO terms were well enriched in cell cycle, DNA replication and DNA repair, where signaling was the main determinant for enrichment by DEGs. CDK2, RAD51, BRCA1 and MCM3 along with many other DEGs that were screened as potential hub genes for neuroblastoma. Our discovery may be useful in exploring the complex molecular mechanism underlying this disease. However, further studies are still required to confirm the significance of our observations.

Acknowledgements

This work was supported by the National Natural Science Foundation of China grants (No.81550031 and No.81201981), Hubei Provincial Health and Family Planning Commission Key Support Project (No.WJ2017Z025), Hubei Provincial Natural Science Foundation Surface project grant (No.2015CFB197), and Talents Innovation, Entrepreneurship and Excellence-creating Project grant of Yichang City, Hubei Province.

Conflict of interests

The authors declare no conflict of interests.

References

1. Louis CU, Shohet JM. Neuroblastoma: Molecular Pathogenesis and Therapy. Annu Rev Med 2015;66:49-63.
2. Jones DTW, Banito A, Grünewald TGP et al. Molecular characteristics and therapeutic vulnerabilities across paediatric solid tumours. Nat Rev Cancer 2019;19:420-38.
3. Zha Y, Xia Y, Ding J et al. MEIS2 is essential for neuroblastoma cell survival and proliferation by transcriptional control of M-phase progression. Cell Death Dis 2014;5:e1417.
4. Matthay KK, Maris JM, Schleiermacher G et al. Nat Rev Dis Primers 2016;2:16078.
5. Pastor ER, Mousa SA. Current management of neuroblastoma and future direction. Crit Rev Oncol Hematol 2019;138:38-43.
6. Geerts D, Revet I, Jorritsma G, Schilderink N, Versteeg R. MEIS homeobox genes in neuroblastoma. Cancer Lett 2005;228:43-50.
7. Vegi NM, Klappacher J, Oswald F et al. MEIS2 Is an

Oncogenic Partner in AML1-ETO-Positive AML. Cell Rep 2016;16:498-507.

8. Lai CK, Norddahl GL, Maetzig T et al. Meis2 as a critical player in MN1-induced leukemia. Blood Cancer J 2017;7:e613.
9. Dumas J, Gargano MA, Dancik GM. shinyGEO: a web-based application for analyzing gene expression omnibus datasets. Bioinformatics 2016;32:3679-3681.
10. Ashburner M, Ball CA, Blake JA et al. Gene ontology: tool for the unification of biology. The Gene Ontology Consortium. Nat Genet 2000;25:25-9.
11. Kanehisa M, Sato Y, Kawashima M, Furumichi M, Tanabe M. KEGG as a reference resource for gene and protein annotation. Nucleic Acids Res 2016;44:D457-62.
12. von Mering C, Huynen M, Jaeggi D, Schmidt S, Bork P, Snel B. STRING: a database of predicted functional associations between proteins. Nucleic Acids Res 2003;31:258-61.
13. Shannon P, Markiel A, Ozier O et al. Cytoscape: a software environment for integrated models of biomolecular interaction networks. Genome Res 2003;13:2498-2504.
14. Stafman LL, Beierle EA. Cell Proliferation in Neuroblastoma. Cancers (Basel) 2016;8. pii: E13.
15. Takagi M, Yoshida M, Nemoto Y et al. Loss of DNA Damage Response in Neuroblastoma and Utility of a PARP Inhibitor. J Natl Cancer Inst 2017;109: doi: 10.1093/jnci/djx062.
16. Koledova Z, Kafkova LR, Calabkova L, Krystof V, Dolezel P, Divoky V. Cdk2 inhibition prolongs G1 phase progression in mouse embryonic stem cells. Stem Cells Dev 2010;19:181-94.
17. Mahajan P, Chashoo G, Gupta M, Kumar A, Singh PP, Nargotra A. Fusion of Structure and Ligand Based Methods for Identification of Novel CDK2 Inhibitors. J Chem Inf Model 2017;57:1957-69.
18. Chen Z, Wang Z, Pang JC et al. Multiple CDK inhibitor dinaciclib suppresses neuroblastoma growth via inhibiting CDK2 and CDK9 activity. Sci Rep 2016;6:29090.
19. Afanasyeva EA, Mestdagh P, Kumps C et al. MicroRNA miR-885-5p targets CDK2 and MCM5, activates p53 and inhibits proliferation and survival. Cell Death Differ 2011;18:974-84.
20. Bhat KP, Cortez D. RPA and RAD51: fork reversal, fork protection, and genome stability. Nat Struct Mol Biol 2018;25:446-53.
21. Chen Q, Cai D, Li M, Wu X. The homologous recombination protein RAD51 is a promising therapeutic target for cervical carcinoma. Oncol Rep 2017;38:767-74.
22. Sarwar R, Sheikh AK, Mahjabeen I, Bashir K, Saeed S, Kayani MA. Upregulation of RAD51 expression is associated with progression of thyroid carcinoma. Exp Mol Pathol 2017;102:446-54.
23. Zhu X, Pan Q, Huang N et al. RAD51 regulates CHK1 stability via autophagy to promote cell growth in esophageal squamous carcinoma cells . Tumour Biol 2016; Oct 14. Doi:10.1007/s13277-016-5455-6 [Epub ahead of print].
24. Seo A, Steinberg-Shemer O, Unal S et al. Mechanism for survival of homozygous nonsense mutations in the tumor suppressor gene BRCA1. Proc Natl Acad Sci U S A 2018;115:5241-6.
25. Nguyen DD, Lee DG, Kim S, Kang K, Rhee JK, Chang S. Integrative Bioinformatics and Functional Analyses of GEO, ENCODE, and TCGA Reveal FADD as a Direct Target of the Tumor Suppressor BRCA1. Int J Mol Sci 2018;19(5). pii: E1458.
26. Li Z, Xu X. Post-Translational Modifications of the Mini-Chromosome Maintenance Proteins in DNA Replication. Genes (Basel) 2019;10(5). pii: E331.
27. Cortez D, Glick G, Elledge SJ. Minichromosome maintenance proteins are direct targets of the ATM and ATR checkpoint kinases. Proc Natl Acad Sci U S A 2004;101:10078-83.